Acta Neuropathol (2017) 134:605–617
DOI 10.1007/s00401-017-1720-z

ORIGINAL PAPER

Sushi repeat-containing protein 1: a novel disease-associated molecule in cerebral amyloid angiopathy

Yasuteru Inoue[1] · Mitsuharu Ueda[1] · Masayoshi Tasaki[1] · Akari Takeshima[2] · Akihito Nagatoshi[1] · Teruaki Masuda[1] · Yohei Misumi[1] · Takayuki Kosaka[1] · Toshiya Nomura[1] · Mayumi Mizukami[1] · Sayaka Matsumoto[1] · Taro Yamashita[1] · Hitoshi Takahashi[2] · Akiyoshi Kakita[2] · Yukio Ando[1]

Received: 12 December 2016 / Revised: 1 May 2017 / Accepted: 1 May 2017 / Published online: 6 May 2017

Abstract Sporadic cerebral amyloid angiopathy (CAA) is characterized by cerebrovascular amyloid beta (Aβ) deposits and causes cerebral hemorrhage and dementia. The exact molecules that co-accumulate with cerebrovascular Aβ deposits are still not fully known. In our study here, we performed proteomic analyses with microdissected leptomeningeal arteries and cerebral neocortical arterioles from 8 cases with severe CAA, 12 cases with mild CAA, and 10 control cases without CAA, and we determined the levels of highly expressed proteins in cerebral blood vessels in CAA. We focused on sushi repeat-containing protein 1 (SRPX1), which is specifically expressed in CAA-affected cerebral blood vessels. Because SRPX1, which is known as a tumor suppressor gene, reportedly induced apoptosis in tumor cells, we hypothesized that SRPX1 may play an important role in Aβ-induced apoptosis in CAA. Immunohistochemical studies revealed that SRPX1 co-accumulated with Aβ deposits in cerebral blood vessels of all autopsied cases with severe CAA. In contrast, no SRPX1 co-accumulated with Aβ deposits in senile plaques. Furthermore, we demonstrated that both Aβ40 and Aβ42 bound to SRPX1 in vitro and enhanced SRPX1 expression in primary cultures of cerebrovascular smooth muscle cells. SRPX1 enhanced caspase activity induced by Aβ40. Knockdown of SRPX1, in contrast, reduced the formation of Aβ40 accumulations and the activity of caspase in cultured cerebrovascular smooth muscle cells. SRPX1 may thus be a novel molecule that is up-regulated in cerebrovascular Aβ deposits and that may increase Aβ-induced cerebrovascular degeneration in CAA.

Keywords Amyloid β · Cerebral amyloid angiopathy · Cerebrovascular degeneration · Cytotoxicity · Proteomics · Sushi repeat-containing protein 1

Abbreviations

AD	Alzheimer's disease
Aβ	Amyloid β
ApoE	Apolipoprotein E
APP	Amyloid precursor protein
BSA	Bovine serum albumin
CAA	Cerebral amyloid angiopathy
CR	Congo red
ELISA	Enzyme-linked immunosorbent assay
HBSS	Hanks' balanced salt solution
HSC-71	Heat shock cognate 71 kDa protein
HRP	Horseradish peroxidase
LCM	Laser capture microdissection
LC–MS/MS	Liquid chromatography–tandem mass spectrometry
PCR	Polymerase chain reaction
SAP	Serum amyloid P component
SRPX1	Sushi repeat-containing protein 1

Introduction

Sporadic cerebral amyloid angiopathy (CAA) is characterized by amyloid beta (Aβ) deposits in leptomeningeal

Electronic supplementary material The online version of this article (doi:10.1007/s00401-017-1720-z) contains supplementary material, which is available to authorized users.

✉ Mitsuharu Ueda
mitt@rb3.so-net.ne.jp

[1] Department of Neurology, Graduate School of Medical Sciences, Kumamoto University, 1-1-1, Chuo-ku, Honjo, Kumamoto-City, Kumamoto 860-8556, Japan

[2] Department of Pathology, Brain Research Institute, Niigata University, Niigata, Japan

vessels, cortical arteries, and capillaries in the brain. Loss of the integrity of cerebral blood vessels caused by intercalation of Aβ into cerebral blood vessels led to spontaneous lobar hemorrhages and dementia in patients with CAA [30]. Postmortem studies revealed that CAA incidences were more than 80 and 70% in patients with Alzheimer's disease (AD) and elderly people, respectively [8, 16].

Several molecules have reportedly co-accumulated with tissue amyloid deposits in patients with amyloidosis. Apolipoprotein E (ApoE) commonly co-accumulated with Aβ deposits in senile plaques in AD. Also, the ε4 genotype of *APOE* was well documented to promote development of AD [12]. The ε2 and ε4 genotypes of *APOE* were both reportedly related to the development and severity of CAA [1, 4, 6]. In addition, serum amyloid P component (SAP) co-accumulated with tissue amyloid deposits and has attracted increasing attention as a target in amyloidosis diagnosis and therapy [23]. In CAA, however, the exact molecules that co-accumulate with cerebrovascular Aβ deposits are still not fully known.

Here, to identify the key molecules in CAA diagnosis and pathogenesis that may lead to therapy for CAA, we used laser capture microdissection (LCM) to perform proteomic analyses with cerebral blood vessels obtained from CAA cases. We investigated highly expressed proteins in these cerebral blood vessels. In the present study, we focused on sushi repeat-containing protein 1 (SRPX1) because of its potential and specific expression in blood vessels as suggested by the human gene expression database available at BioGPS (http://biogps.org), which provides the highest SRPX1 mRNA levels in smooth muscle among various human tissue sites. Also, because SRPX1, which is known as a tumor suppressor gene, reportedly induced apoptosis in tumor cells [26, 27], we hypothesized that SRPX1 may play an important role in Aβ-induced apoptosis in CAA. Furthermore, previous studies had not indicated that SRPX1 associated with the other form of Aβ deposits in senile plaques of AD brains [7, 15]. SRPX1, a transmembrane protein consisting of 464 amino acids, has three sushi domains, which are found in various kinds of complement and adhesion proteins [13]; it also has a short intracellular domain in the C-terminal region [22, 25–27]. *SRPX1* was initially identified as a causative gene in patients with X-linked retinitis pigmentosa [17]. Expression of SRPX1 mRNA was reportedly down-regulated in tumor cells, and the *SRPX1* gene was thought to be a tumor suppressor gene [14, 25–27]. *SRPX2*, a paralog of *SRPX1*, was reportedly involved in angiogenesis, cell adhesion, and synapse formation. Recent studies also suggested that the C-terminal regions of those SRPXs may be involved in redox-dependent regulation [22]. In our study here, we demonstrated that SRPX1 bound to Aβ in vitro and that SRPX1 enhanced the cytotoxic effects of Aβ in primary cultured cerebrovascular smooth muscle cells.

Materials and methods

Patients and sample collection

We studied 55 consecutive cases, autopsied at Kumamoto University Hospital from 1990 to 2012, for which brain tissue samples were available. Autopsies had been performed on cases aged 50 years or older (4 cases in their 50s, 18 in their 60s, 21 in their 70s, 11 in their 80s, and 1 in her 90s). To determine the occurrence of CAA, we studied cerebral neocortical tissues in each case (Supplementary Table S1). In addition, we used occipital cortex tissues obtained from five randomly selected cases with severe CAA and five control non-CAA cases autopsied at the Brain Research Institute, Niigata University, Niigata, Japan (Supplementary Table S1).

The pathological staging of neurofibrillary tangles was assessed according to the modified Braak neuropathological staging system of Alzheimer-related changes [3]. The burden of neuritic plaques in the cortical section was evaluated according to the criteria of the Consortium to Establish a Registry for Alzheimer's disease (CERAD) [18]. Supplementary Table S1 provides clinicopathological information about the autopsied cases, and the control cases, used in this study. Supplementary Fig. S1 presents a flow chart illustrating sample collection and the inclusion criteria.

For proteomic analyses, we used cerebral neocortical tissues obtained from cases with severe CAA ($n = 8$) or mild CAA ($n = 12$) and cerebral neocortical tissues from randomly selected age-matched control subjects without CAA ($n = 10$). To investigate SRPX1 mRNA levels, we used frozen occipital cortex tissues dissected from randomly selected control subjects ($n = 5$).

Congo red (CR) staining and immunohistochemical staining

We performed CR staining and immunohistochemical staining with formalin-fixed, paraffin-embedded consecutive brain sections as described previously [29]. Brain tissues were stained with an anti-human Aβ/amyloid precursor protein (APP) antibody (pretreated with formic acid) (1:100 dilution, clone 6F/3D; DAKO, Glostrup, Denmark), an anti-human SRPX1 antibody (pretreated by autoclaving at 120 °C for 20 min in citric acid buffer) (1:100 dilution; Atlas Antibodies, Stockholm, Sweden), or an anti-phospho tau antibody (AT8, 1:200 dilution; Thermo Fisher Scientific, Waltham, MA). Secondary antibodies conjugated with

horseradish peroxidase (HRP) (1:100, DAKO) were used for visualization of immunoreactive lesions by means of the ImmPACT DAB peroxidase substrate (Vector Laboratories, Burlingame, CA), followed by counterstaining with hematoxylin. For selective staining of Aβ40, we used the Amyloid β-protein immunohistostain kit (WAKO Pure Chemical Industries Ltd., Osaka, Japan).

For immunofluorescence studies, sections were blocked with 10% goat serum in PBS buffer-containing 0.2% Triton-X-100 and were incubated overnight with following primary antibodies: anti-human collagen IV (1:100 dilution; Chemicon, Temecula, CA), monoclonal antibody against α-smooth muscle actin (1:200 dilution; Sigma-Aldrich, St. Louis, MO), or anti-CD31 (1:20 dilution; DAKO). For these immunofluorescence studies, Alexa Fluor 594 goat anti-mouse IgG, Alexa Fluor 488 goat anti-rabbit, and Alexa Fluor 594 donkey anti-mouse (1:100 dilution; Invitrogen, Carlsbad, CA) were used as secondary antibodies. The samples were mounted by applying Vectashield Mounting Medium (Vector Laboratories) and were visualized using a fluorescence microscope (BZ-X700; Keyence, Osaka, Japan).

Three trained observers who were blinded to the clinical information independently assessed the histopathological findings.

Protein extraction and proteome analysis

We performed protein extraction and proteome analysis using liquid chromatography coupled with tandem mass spectrometry (LC–MS/MS), as previously described [28, 31]. Briefly, leptomeningeal and cortical vessels were isolated via LCM from 8 cases with severe CAA with extensive circumferential deposition of Aβ, 12 cases with mild CAA with a small amount of Aβ deposition, and 10 control subjects without CAA. LCM (LMD7000; Leica Microsystems, Wetzel, Germany) was performed using the bright-field setting to confirm the presence of cerebrovascular lesions, which were placed into microcentrifuge tubes containing 10 mM Tris, 1 mM EDTA, and 0.002% Zwittergent 3–16. Collected tissue samples were heated at 98 °C for 90 min. Samples were sonicated for 90 min and digested with 1.5 μl of 1 mg/ml trypsin (Promega, Madison, WI) overnight at 37 °C. Digested peptide mixtures were analyzed using nano-flow reversed-phase LC–MS/MS (LTQ Velos Pro; Thermo Fisher Scientific). We obtained the relative abundances of the identified molecules using the normalized spectral abundance factor [21].

Binding of Aβ40 and Aβ42 to SRPX1 in vitro

To determine the binding ability of Aβ40 and Aβ42 to SRPX1 in vitro, we performed an enzyme-linked immunosorbent assay (ELISA) as described earlier [9]. Briefly, after coating the anti-human SRPX1 antibody (1:200 dilution) in bicarbonate/carbonate coating buffer (100 mM, pH 9.5) at 4 °C overnight, 1 μM recombinant SRPX1 (Proteintech, Chicago, IL) was added as the capture antigen; 1% bovine serum albumin (BSA) was used as the negative control. Various concentrations (0–1.0 μM) of native Aβ40 or Aβ42 were added and then incubation proceeded with the anti-human Aβ/APP antibody (1:10,000 dilution, clone 6E10; Biolegend, San Diego, CA). After incubation with an HRP-conjugated secondary antibody and color development, the absorbance at 450 nm was measured with a microplate spectrophotometer (Bio-Rad, Hercules, CA).

Knockdown of SRPX1 by siRNA

Primary murine cerebrovascular smooth muscle cells isolated from 3-month-old C57BL/6 J mice were cultured according to a previous report [10]. To knock down SRPX1 expression, we transfected primary cerebrovascular smooth muscle cells with SRPX1-specific siRNA (MISSION esiRNA; Sigma-Aldrich) complexed with Lipofectamine RNAi Max (Invitrogen) in Opti-MEM (Gibco, Grand Island, NY) for 48 h, according to the manufacturer's protocol. Luciferase siRNA (MISSION esiRNA; Sigma-Aldrich) served as the negative control siRNA.

Treatment of murine cerebrovascular smooth muscle cells with Aβ

Primary cultured murine cerebrovascular smooth muscle cells were treated with freshly prepared Aβ40 or Aβ42, at a final concentration of 10 μM, for 24 h. The same volume of PBS was used as a negative control. Hydrogen peroxide, at final concentrations of 100–1000 nM, was also used as a control agent for 24 h. To detect Aβ deposits in cultured cells, we performed immunohistochemistry with anti-human Aβ antibody (1:100 dilution, clone 6F/3D; DAKO). Oligomerization of Aβ was analyzed via glutaraldehyde cross-linking and Western blotting with the anti-human Aβ/APP antibody (1:1000 dilution, clone 6E10; Biolegend).

Determination of caspase-3/7 activity

Caspase-3/7 activity was determined in cultured smooth muscle cells treated with Aβ40 at a final concentration of 10 μM for 24 h using the Apo-ONE Homogeneous Caspase-3/7 Assay (Promega), according to the manufacturer's instructions. Fluorescence was measured with the Filter-Max F5 Microplate Reader (Molecular Devices, Sunnyvale, CA).

Real-time quantitative reverse transcription polymerase chain reaction (PCR)

We extracted total RNA from primary cultures of murine cerebrovascular smooth muscle cells using the RNeasy Mini Kit (Qiagen, Hilden, Germany). We also extracted total RNA from human and murine cerebral cortex, hippocampus, and purified cerebral blood vessels using the TRIzol reagent (Thermo Fisher Scientific). We isolated cerebral blood vessels according to the method of Boulay et al. while allowing for mechanical isolation [2]. Briefly, brain tissues obtained from human cases (see Supplementary Table S1) and from 3-month-old C57BL/6 J male mice were homogenized in Hanks' balanced salt solution (HBSS) buffer supplemented with 10 mM HEPES, followed by centrifugation at 2000×*g* for 10 min at 4 °C. The precipitates were resuspended in 18% dextran in HBSS buffer and centrifuged at 4400×*g* for 15 min at 4 °C. The final pellets were resuspended in 2 ml of HBSS buffer and were passed through a 40-μm nylon mesh (BD Biosciences, San Jose, CA). We used cerebral blood vessels retained on the mesh for real-time PCR analyses.

Real-time PCR was performed as previously described [19]. Primers used were as follows: mouse SRPX1 forward: 5′-GATCAGAGCAAAGATTATGCCT CCA-3′; mouse SRPX1 reverse: 5′-CTTTATCCATG CCATGCTTATCCA-3′; mouse GAPDH forward: 5′-TTAGCACCCCTGGCCAAGG-3′; mouse GAPDH reverse: 5′- CTTACTCCTTGGAGGCCATG-3′; human SRPX1 forward: 5′-GCCATGCCAGCAAATGGAG-3′; human SRPX1 reverse: 5′-ACACTTGGGCACTTGA TTCTAGGAG-3′; human GAPDH forward: 5′- GAGT CAACGGATTTGGTCGT-3′; human GAPDH reverse: 5′- TTGATTTTGGAGGGATCTCG-3′.

Western blot analysis

Primary cultured murine cerebrovascular smooth muscle cells were washed twice in ice-cold PBS and then lysed by the addition of RIPA buffer (Thermo Fisher Scientific) containing freshly added protease inhibitor cocktail (Nacalai Tesque, Kyoto, Japan). Protein concentrations were determined using the BCA Protein Assay kit (Pierce Chemical, Rockford, IL), and equal amounts of protein from each sample were resolved by means of 10% SDS-PAGE and transferred to PVDF membranes (Bio-Rad). We performed Western blot analysis as previously described [19]. Briefly, the PVDF membranes containing the proteins were first incubated with a blocking buffer (Blocking One; Nacalai Tesque) and were then incubated with an anti-mouse SRPX1 antibody (1:4000 dilution; ProSci, Poway, CA) or an anti-mouse GAPDH antibody (1:1000 dilution; MBL, Nagoya, Japan) followed by incubation with an HRP-conjugated secondary antibody. We used ImageJ 1.47 software (NIH, Bethesda, MD) to analyze the intensity of specific bands.

APOE genotyping

Genomic DNA was extracted from the formaldehyde-fixed paraffin-embedded brain tissues according to the manufacturer's instructions (QIAamp DNA FFPE Tissue Kit; Qiagen, Düsseldorf, Germany) [24]. *APOE* genotyping was performed using a semi-nested PCR assay followed by digestion with the restriction enzyme *Hha*I as described previously [11].

Statistical analysis

We analyzed data via Student's *t* test and one-way ANOVA followed by Tukey's post hoc test when the ANOVA reached significance. A non-parametric test (Mann–Whitney *U* test) was used for mass spectrometric analyses. The level of statistical significance was set at $p < 0.05$. Statistical analyses were performed using JMP 9.0 statistical software (SAS Institute, Cary, NC).

Ethics

The Human Ethics Review Committee of Kumamoto University approved the study protocol. Families of subjects provided signed consent forms. All patients' family members gave informed consent for performance of an autopsy. The Animal Care and Use Committee of Kumamoto University School of Medicine approved the protocols for animal experiments.

Results

Up-regulated molecules in autopsied CAA cases

In our postmortem analyses, the occurrence of CAA was 27.3% ($n = 15$), with the value increasing with age (the trend being 0, 5.6, 38.1, and 50.0% for patients who had had autopsies in their 50s, 60s, 70s, and 80s and older, respectively, $p = 0.017$) (Supplementary Fig. S2). The occurrence of senile plaques was 60.0% ($n = 33$) in those autopsied cases. Genotype frequencies for cases with CAA differed from frequencies for cases without CAA (Table 1).

Table 1 Clinicopathological characteristics of autopsied cases with and without CAA

Feature	Without CAA ($n = 45$)	With CAA ($n = 20$)	p value
Age, years (mean ± SD)	70 ± 9	78 ± 7	<0.001
Males/females	24/21	11/9	0.901
Hypertension	20 (44)	5 (25)	0.137
Diabetes mellitus	6 (13)	2 (10)	0.706
Dyslipidemia	3 (7)	1 (5)	0.796
Alcohol consumption	16 (36)	8 (40)	0.733
Smoking habit	15 (33)	6 (30)	0.791
Accumulation of SRPX1 in cerebral blood vessels	17 (38)	17 (85)	<0.001
Presence of senile plaque	24 (53)	16 (80)	0.041
ApoE genotypes[a]			0.047*
ε2/ε2	0 (0)	0 (0)	
ε2/ε3	1 (3)	2 (13)	
ε2/ε4	2 (5)	0 (0)	
ε3/ε3	27 (68)	5 (33)	
ε3/ε4	10 (25)	8 (53)	
ε4/ε4	0 (0)	0 (0)	
Braak AD tau stage (0–II/III–IV/V–VI)	38/6/1	8/5/7	<0.001*
CERAD score (0/A/B/C)	21/19/4/1	4/6/3/7	<0.01*

Data are presented as numbers of patients with percentages in parentheses

* p values for trends across groups

[a] ApoE genotyping was performed in 55 autopsied cases

We performed proteomic analyses with microdissected cerebrovascular tissue samples and identified the up-regulated molecules in the cerebral blood vessels of severe CAA cases (Table 1). Six molecules, Aβ, ApoE, glial fibrillary acidic protein (GFAP), two isozymes (α and β) of enolase, and SRPX1, were significantly up-regulated in severe CAA cases, and those molecules were detected in all eight cases with severe CAA (Table 2). In the present study, we focused on SRPX1 because of its potential specific expression in blood vessels. In addition, because SRPX1, which is known as a tumor suppressor gene, reportedly induced apoptosis in tumor cells [26, 27], we hypothesized that SRPX1 may play an important role in Aβ-induced apoptosis in CAA. Our proteomic analyses also revealed that SRPX1 levels in cerebral blood vessels of severe CAA cases were higher than those of mild CAA cases (Supplementary Table S2). Although we did not find SRPX1 up-regulation in mild CAA cases compared with control non-CAA cases by means of proteomic analyses (Supplementary Table S3), immunohistochemical staining, which is thought to be a more sensitive method for detecting SRPX1 in cerebral blood vessels, revealed that SRPX1 was indeed up-regulated in mild CAA cases compared with control non-CAA cases (Fig. 1).

Accumulation and Aβ binding of SRPX1 in cerebral blood vessels in autopsied cases with and without CAA and in mouse brain

Immunohistochemical studies revealed that SRPX1 co-accumulated with Aβ amyloid deposits in cerebral blood vessels of autopsied cases with CAA (Fig. 1a–e). In contrast, SRPX1 did not co-accumulate with Aβ deposits in senile plaques (Fig. 1e). SRPX1 accumulated in cerebral blood vessels in cases with CAA significantly more often than in those without CAA (Fig. 1f–k, Table 1). The percentages of SRPX1-positive vessels were significantly higher for both leptomeningeal arteries (≥100 μm in diameter) (Fig. 1f) and leptomeningeal arterioles (<100 μm in diameter) (Fig. 1g) in CAA cases compared with control non-CAA cases. In cortical arteries, the percentages of SRPX1-positive vessels were not different in both CAA and non-CAA cases (Fig. 1h). SRPX1 accumulation was not found in white matter vessels (Supplementary Fig. S3). SRPX1 was frequently found in the basement membrane

Table 2 Significantly up-regulated molecules in cerebral blood vessels of cases with severe CAA

Accession number	Protein	Severe CAA ($n = 8$)[a]		Control ($n = 10$)[a]		Relative value of $NSAF_{CAA/Control}$	p value*
		Detection ratio (%)	$NSAF_{CAA}$	Detection ratio (%)	$NSAF_{Control}$		
P05067	Amyloid beta	100	4.890	0	ND	NA	<0.0001
P06733	Alpha-enolase	100	3.503	0	ND	NA	<0.0001
P13929	Beta-enolase	100	3.045	20	0.179	17.0	0.0004
P02649	Apolipoprotein E	100	7.847	60	0.347	22.6	0.0004
P14136	Glial fibrillary acidic protein	100	3.045	30	0.302	10.1	0.0008
P78539	SRPX1	100	0.938	40	0.247	3.8	0.0133
P09972	Fructose-bisphosphate aldolase C	88	1.545	60	0.385	4.0	0.0149
P04004	Vitronectin	88	1.072	80	0.335	3.2	0.0276
P30086	Phosphatidylethanolamine-binding protein 1	88	1.471	80	0.749	2.0	0.0335
P43003	Excitatory amino acid transporter 1	75	0.176	0	ND	NA	0.0013
P10909	Clusterin	75	2.438	10	0.144	16.9	0.0047
P27105	Erythrocyte band 7 integral membrane protein	75	1.103	20	0.197	5.6	0.0189
Q16555	Dihydropyrimidinase-related protein 2	75	0.677	30	0.122	5.5	0.0196
Q8NCH0	Carbohydrate sulfotransferase 14	75	0.366	30	0.080	4.6	0.0208
Q01082	Spectrin beta chain, brain 1	75	0.069	40	0.019	3.7	0.0368
P16152	Carbonyl reductase [NADPH] 1	75	0.677	40	0.217	3.1	0.0489
O14773	Tripeptidyl-peptidase 1	63	0.195	0	ND	NA	0.0043
P21741	Midkine	63	1.311	0	ND	NA	0.0049
Q9NRN5	Olfactomedin-like protein 3	63	0.712	10	0.026	27.5	0.0128
P09471	Guanine nucleotide-binding protein G(o) subunit alpha	63	0.565	10	0.028	20.0	0.0168
P04003	C4b-binding protein alpha chain	63	0.168	10	0.017	10	0.0190
Q15084	Protein disulfide-isomerase A6	63	0.142	10	0.023	6.2	0.0225
P15311	Ezrin	63	0.192	10	0.034	5.6	0.0376
P23297	Protein S100-A1	50	0.532	0	ND	NA	0.0137
P40121	Macrophage-capping protein	50	0.144	0	ND	NA	0.0137
P56705	Protein Wnt-4	50	0.178	0	ND	NA	0.0143
Q92765	Secreted frizzled-related protein 3	50	0.192	0	ND	NA	0.0143
Q15435	Protein phosphatase 1 regulatory subunit 7	50	0.316	0	ND	NA	0.0143
Q13813	Spectrin alpha chain, non-erythrocytic 1	50	0.041	0	ND	NA	0.0146

Table 2 continued

Accession number	Protein	Severe CAA ($n = 8$)[a]		Control ($n = 10$)[a]		Relative value of $NSAF_{CAA/Control}$	p value*
		Detection ratio (%)	$NSAF_{CAA}$	Detection ratio (%)	$NSAF_{Control}$		
Q149N8	E3 ubiquitin-protein ligase	50	0.053	0	ND	NA	0.0146
P80723	Brain acid soluble protein 1	50	1.026	10	0.058	17.7	0.0430
P01008	Antithrombin-III	50	0.332	10	0.022	15.4	0.0430
P07093	Glia-derived nexin	38	0.094	0	ND	NA	0.0393
O75094	Slit homolog 3 protein	38	0.026	0	ND	NA	0.0393
P49368	T-complex protein 1 subunit gamma	38	0.074	0	ND	NA	0.0393
P33793	DNA polymerase	38	0.037	0	ND	NA	0.0393
Q14894	Thiomorpholine-carboxylate dehydrogenase	38	0.119	0	ND	NA	0.0393
P04156	Major prion protein	38	0.152	0	ND	NA	0.0393
Q66K79	Carboxypeptidase Z	38	0.088	0	ND	NA	0.0400
Q9UHG2	ProSAAS	38	0.240	0	ND	NA	0.0400
Q99798	Aconitate hydratase, mitochondrial	38	0.064	0	ND	NA	0.0400
P26572	Alpha-1,3-mannosyl-glycoprotein 2-beta-N-acetylglucosaminyltransferase	38	0.169	0	ND	NA	0.0402

ND not detected, *NA* not applicable

* The Mann–Whitney *U* test was used for comparisons between $NSAF_{CAA}$ and $NSAF_{Control}$ values

[a] Protein abundance values were estimated using NSAF (normalized spectral abundance factor) normalization

of cerebral blood vessels in both mild and severe CAA cases (Fig. 1l–n, Supplementary Table S4). The percentages of SRPX1-positive endothelial cells tended to be higher in severe CAA cases than in mild CAA cases (Supplementary Table S4, Supplementary Fig. S4).

Real-time PCR analyses revealed significantly higher SRPX1 mRNA expression in isolated cerebral blood vessels than in the cerebral cortex and hippocampus in mice (Fig. 2a). In human brain samples, SRPX1 mRNA levels in cerebral blood vessels isolated from the cortex region were also significantly higher than tissue levels in the cortex obtained from the same cases (Fig. 2b).

We investigated the binding of Aβ40 and Aβ42 to SRPX1 using an ELISA with surfaces coated with SRPX1. Both Aβ40 and Aβ42 bound to SRPX1 in a concentration-dependent manner (ranging from 0.1 to 1.0 μM) but did not bind to the control protein 1% BSA (Fig. 3a, b).

Reduction of Aβ40 accumulations by SRPX1 knockdown in primary cultures of cerebrovascular smooth muscle cells

siRNA targeting SRPX1 reduced SRPX1 mRNA and protein levels to 30.3 and 37.4%, respectively, in primary cultures of murine cerebrovascular smooth muscle cells (Fig. 3c, d, Supplementary Fig. S5). We added freshly prepared Aβ peptides to the culture medium of cultured cells treated with siRNAs at a final concentration of 10 μM for 24 h and found Aβ accumulations in the cells using immunohistochemical analysis with anti-human Aβ/APP antibody. Aβ accumulations were reduced in cultured cerebrovascular smooth muscle cells treated with SRPX1 siRNA compared with cultured cells treated with control siRNA (Fig. 3e, f). The Aβ that was added to the cultured cells formed oligomeric aggregates in the cultured cells after 24 h (Supplementary Fig. S6).

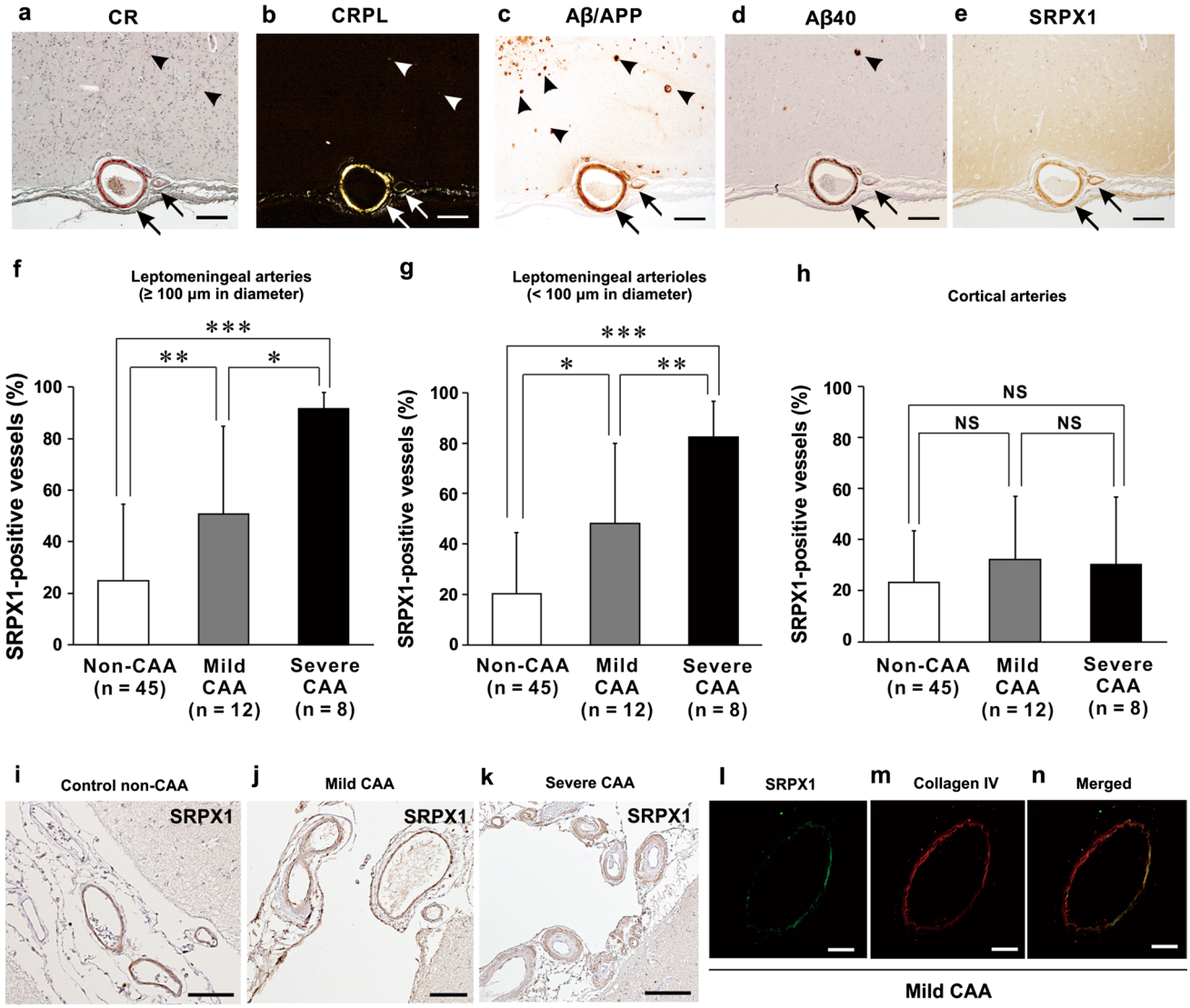

Fig. 1 Representative histopathological images from a case with severe CAA (case no. SC-4). Serial sections show CR-positive leptomeningeal arteries surrounding the occipital cortex (**a**) and those same arteries viewed under polarized light (CRPL) (**b**). These arteries stained positive for Aβ/APP (**c**), Aβ40 (**d**), and SRPX1 (**e**) (*arrows*). An Aβ-stained brain parenchymal lesion revealed that senile plaques were negative for SRPX1 (**a–f**). *Arrowheads* point to senile plaques. *Scale bars* 200 μm in **a–e**. **f–h** *Percentages* of SRPX1-positive cerebral blood vessels in autopsied cases with mild or severe CAA and in autopsied cases without CAA (*control*). Leptomeningeal arteries (≥100 μm in diameter) (**f**), leptomeningeal arterioles (<100 μm in diameter) (**g**), and cortical arteries (**h**). $*p < 0.05$, $**p < 0.01$, $***p < 0.001$. *NS* not significant. **i–k** Representative cerebrovascular SRPX1-positive images from a control non-CAA case (case no. C-17) (**i**), a mild CAA case (case no. MC-11) (**j**), and a severe CAA case (case no. SC-3) (**k**). *Scale bars* 100 μm in **i–k**. **l–n** Early accumulation of SRPX1 (**l**) in the collagen IV-positive (**m**) basement membrane of cerebral blood vessels in a mild CAA case (case no. MC-6). **n** Merged image for SRPX1 (*green*) and collagen IV (*red*). *Scale bars* 100 μm in **l–n**

Induction of SRPX1 expression by Aβ40 and Aβ42 in primary cultures of cerebrovascular smooth muscle cells

To investigate whether Aβ40 and Aβ42 could induce SRPX1 expression in primary cultures of cerebrovascular smooth muscle cells, we examined SRPX1 mRNA and protein levels in cultured smooth muscle cells treated with Aβ at a final concentration of 10 μM for 24 h and in cells that were not treated. Both Aβ40 and Aβ42 significantly increased the SRPX1 mRNA level and protein expression (Fig. 4a, b). We used hydrogen peroxide as a control toxic agent in the cell culture studies. A low concentration (100 nM) of hydrogen peroxide did not affect

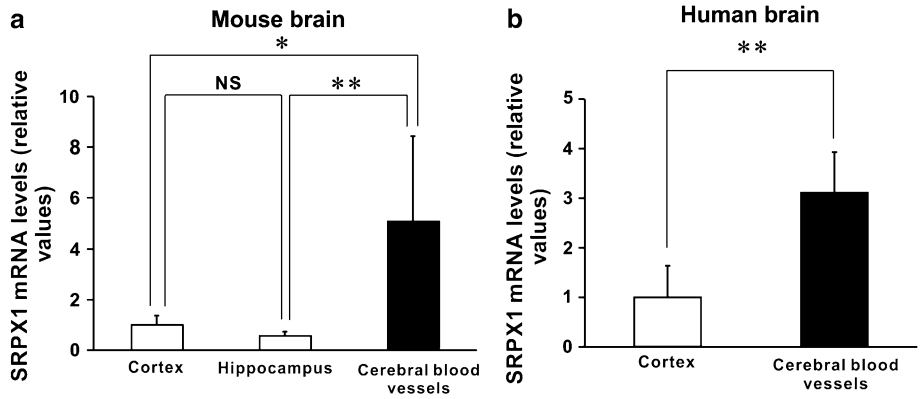

Fig. 2 SRPX1 mRNA levels in cerebral cortex tissues and blood vessels. **a** SRPX1 mRNA levels in the cerebral cortex, hippocampus, and cerebral blood vessels from 3-month-old C57BL/6 J male mice ($n = 3$). **b** SRPX1 mRNA levels in human cortex tissues and isolated cerebral blood vessels obtained from autopsied cases ($n = 5$). SRPX1 mRNA levels were normalized to GAPDH mRNA. Data represent mean ± SEM. *NS* not significant. *$p < 0.05$, **$p < 0.01$

SRPX1 expression, but a high concentration (500 nM) reduced SRPX1 expression in cultured cerebrovascular smooth muscle cells (Supplementary Fig. S7a).

Augmentation of caspase 3/7 activity by concomitant administration of SRPX1 and Aβ40

Aβ40 induced caspase-3/7 activity in primary cultures of murine cerebrovascular smooth muscle cells. Although SRPX1 alone did not induce caspase-3/7 activity in these cells, concomitant administration of SRPX1 and Aβ40 enhanced caspase-3/7 activity, which was significantly greater than that induced by a single administration of Aβ40 in primary cultures of cerebrovascular smooth muscle cells (Fig. 5a). Knockdown of SRPX1 significantly reduced caspase-3/7 activity induced by Aβ40 (Fig. 5b).

We used hydrogen peroxide as a control toxic agent in the cell culture studies. A low concentration (100 nM) of hydrogen peroxide did not affect caspase-3/7 activity, whereas a high concentration (500 nM) induced increased caspase-3/7 activity in cultured cerebrovascular smooth muscle cells (Supplementary Fig. S7b).

Discussion

In the present study, we identified up-regulated molecules, including SRPX1, in cerebral blood vessels in CAA cases by means of proteomic analyses. Because SRPX1, which is known as a tumor suppressor gene, reportedly induced apoptosis in tumor cells [26, 27], we hypothesized that SRPX1 may play an important role in Aβ-induced apoptosis in CAA. We found significant up-regulation of SRPX1 in cerebral blood vessels in CAA cases. Furthermore, our in vitro analyses revealed that SRPX1 bound to Aβ and enhanced Aβ cytotoxicity in cultured cerebrovascular smooth muscle cells.

We first found that SRPX1 co-accumulated with cerebrovascular Aβ amyloid deposits in CAA and bound to Aβ in vitro but did not co-accumulate with Aβ in senile plaques, which is another important form of Aβ amyloid deposits in the cerebral cortex and hippocampus. We also found significant expression of SRPX1 in cerebral blood vessels, more than in the cerebral cortex. Higher expression of SRPX1 in cerebral blood vessels may contribute to specific accumulation of SRPX1 in cerebrovascular Aβ amyloid deposits in CAA. Our immunohistological studies revealed that SRPX1 frequently accumulated in the basement membrane of cerebral blood vessels in mild CAA cases, similar to the formation of Aβ deposits. This result suggests that the accumulation of SRPX1 may be an early event in CAA. In addition, the percentages of SRPX1-positive vessels were significantly higher in severe CAA cases compared with mild CAA cases in both proteomic and immunohistological analyses. SRPX1 may thus contribute to enhancing both early and late phases of CAA.

Second, we determined that Aβ up-regulated SRPX1 expression in cerebrovascular smooth muscle cells. Expression of SRPX1 mRNA was reportedly down-regulated in tumor cells, and the *SRPX1* gene was thought to be a tumor suppressor gene [14, 25–27]. SRPX1 also induced apoptosis in human tumor cells [14, 25–27]. In the present study, we found that SRPX1 significantly enhanced apoptosis induced by Aβ40 in cerebrovascular smooth muscle cells. In contrast, knockdown of SRPX1

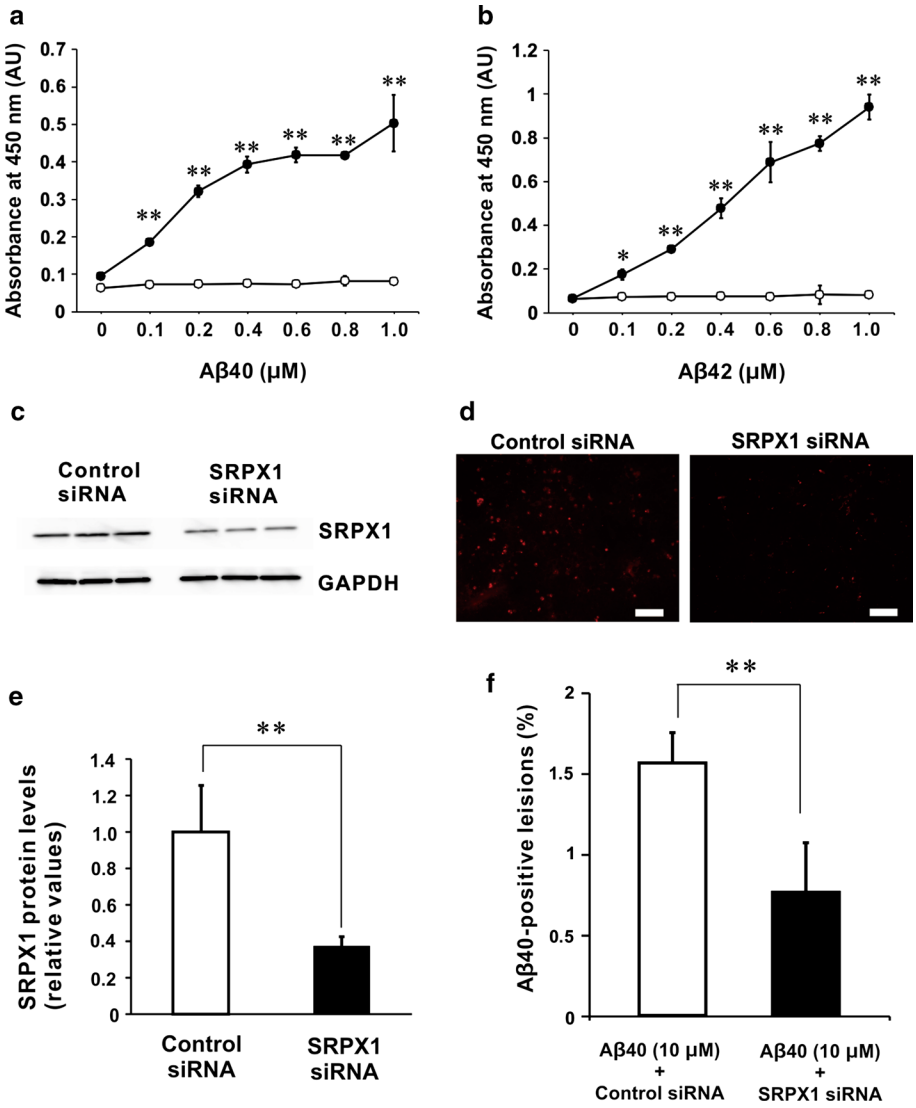

Fig. 3 Aβ binding of SRPX1. ELISA results for the binding ability of Aβ40 (**a**) and Aβ42 (**b**) to SRPX1 in vitro. *White circles* indicate the amount of Aβ on antigen-free surfaces, and *black circles* indicate the amount of Aβ40 on surfaces coated with SRPX1 (1 μM). $*p < 0.005$, $**p < 0.001$, surfaces coated with SRPX1 versus control surfaces. **c** Representative *Western blots* of cell lysates of cultured cerebrovascular smooth muscle cells, which were treated with control siRNA or SRPX1 siRNA for 48 h and analyzed using anti-SRPX1 and anti-GAPDH antibodies. **d** Quantified SRPX1 protein levels in the Western blots of cell lysates of cultured cerebrovascular smooth muscle cells treated with control siRNA or SRPX1 siRNA. Data were normalized to GAPDH. $**p < 0.05$ versus control. **e** Formation of Aβ accumulations in cultured murine cerebrovascular smooth muscle cells treated with Aβ40 at a final concentration of 10 μM for 24 h with control siRNA or SRPX1 siRNA. Immunofluorescence studies with anti-human Aβ/APP antibody (1:100 dilution, clone 6F/3D; DAKO) in cultured cells treated with control siRNA or SRPX1 siRNA. *Scale bars* 100 μm. **f** Percentages of Aβ40-positive lesions were quantified by averaging ten random fields for cultured cells treated with control siRNA or SRPX1 siRNA. Data represent mean ± SEM from three independent experiments. $**p < 0.01$

reduced Aβ40-induced apoptosis. Because we found that SRPX1 bound to Aβ, to support the binding interaction we used siRNA to knock down SRPX1 expression in murine cerebrovascular smooth muscle cells. We found reduced Aβ accumulations compared with the result with control siRNA. SRPX1 may play a role in the deposition

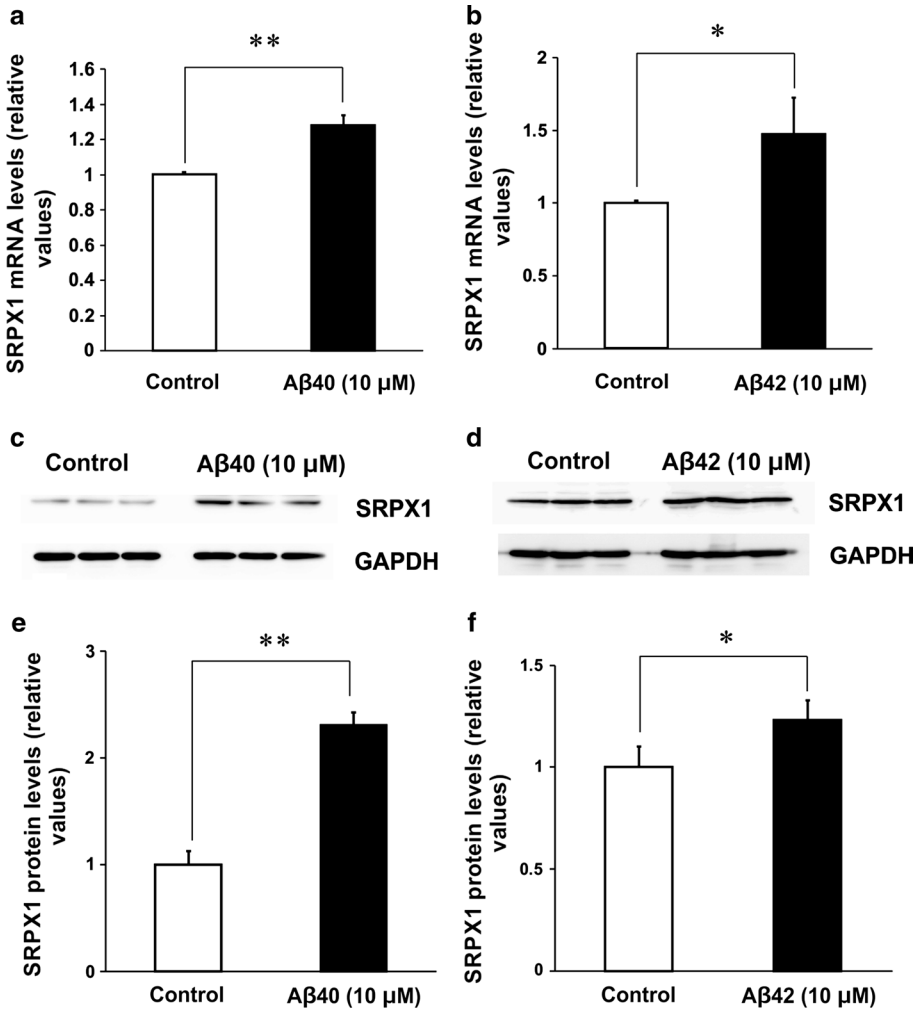

Fig. 4 SRPX1 mRNA levels in primary cultured murine cerebrovascular smooth muscle cells treated with Aβ40 (**a**) or Aβ42 (**b**) at a final concentration of 10 μM for 24 h and in cells without such treatment. SRPX1 mRNA levels were normalized to GAPDH mRNA levels. *$p < 0.05$, **$p < 0.01$ versus control. **c**, **d** Representative Western blots of cell lysates of cultured cerebrovascular smooth muscle cells, which were treated with Aβ40 (**c**) or Aβ42 (**d**) at a final concentration of 10 μM for 24 h, or were not treated (*Control*), as analyzed using anti-SRPX1 and anti-GAPDH antibodies. **e**, **f** Quantified SRPX1 protein levels in the Western blots of cell lysates of cultured cerebrovascular smooth muscle cells treated with Aβ40 (**e**) or Aβ42 (**f**) or not treated (*Control*). Data were normalized to GAPDH. *$p < 0.05$, **$p < 0.01$ versus control

of Aβ on the cell surface through its binding ability with Aβ and thus enhance Aβ-induced cerebrovascular degeneration in CAA. A potential limitation of this study is that the role of SRPX1 remains to be fully elucidated in cerebrovascular endothelial cells in CAA. Because our immunohistological analyses revealed that SRPX1 was also expressed in cerebrovascular endothelial cells, especially in severe CAA cases, SRPX1 may also play important roles in cerebrovascular endothelial cells in CAA. Further studies are needed to clarify this issue.

Our proteomic analyses also determined that other molecules, including ApoE, enolase, GFAP, vitronectin, clusterin, and midkine, were significantly up-regulated in cerebral blood vessels in CAA cases. Most of those up-regulated molecules were also found in AD brains [5, 7, 15, 20]. Those molecules may play roles in the formation of both vascular Aβ deposits in CAA and senile plaques in AD, and may therefore serve some functions in pathogenic pathways in CAA and AD.

On the basis of the findings just detailed, SRPX1 may be a novel molecular target in CAA diagnosis and therapy. Scintigraphy detecting another well-known co-accumulating molecule in amyloid deposits, SAP, is currently used to diagnose amyloidosis [23]. Scintigraphy with a novel co-accumulating molecule in cerebrovascular Aβ amyloid deposits, SRPX1, may therefore be a new diagnostic tool for CAA. In addition, inhibition of SRPX1 may be a novel therapeutic target to reduce Aβ-induced cerebrovascular degeneration in CAA. To pursue this issue, we must conduct additional in vivo studies.

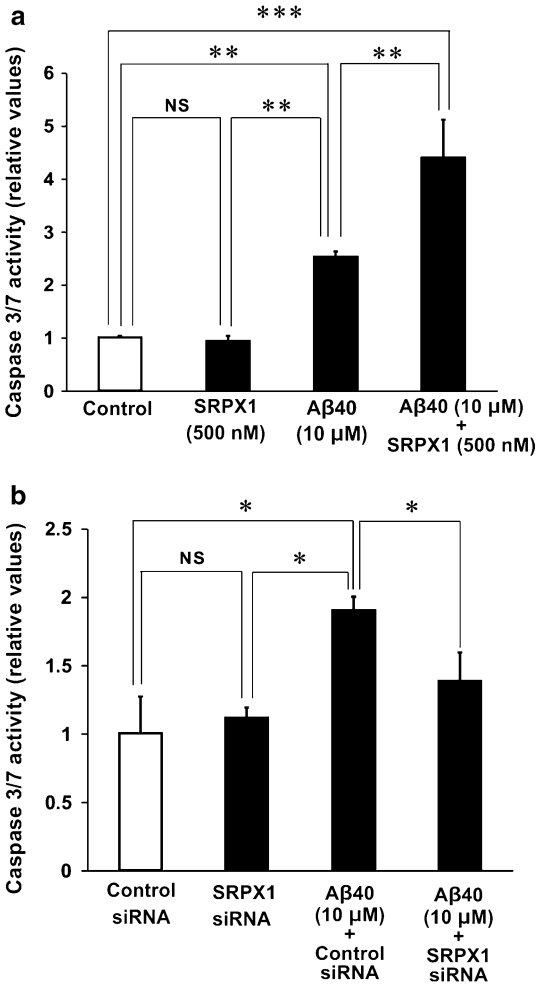

Fig. 5 **a** Caspase-3/7 activity in cerebrovascular smooth muscle cells. Enhancement of caspase-3/7 activity by concomitant administration of SRPX1 and Aβ40. **b** Reduction of Aβ40-induced caspase-3/7 activity by SRPX1 knockdown. Data represent mean ± SEM from three independent experiments. *$p < 0.05$, **$p < 0.01$. *NS* not significant

In conclusion, SRPX1 may be a novel molecule that is associated with CAA and may enhance Aβ-induced cerebrovascular degeneration in CAA.

Acknowledgements We express our gratitude to Ms. Hiroko Katsura for her technical support during histopathological investigations. We are indebted to Ms. Judith B. Gandy for providing professional English editing of the manuscript.

Compliance with ethical standards

Funding This research was supported by Grants-in-Aid for Science Research from the Ministry of Education, Culture, Sports, Science and Technology of Japan (Grant Numbers 15K09318, 15H04841, 15K15195).

Conflict of interest The authors have no conflicts of interest to disclose.

References

1. Biffi A, Sonni A, Anderson CD, Kissela B, Jagiella JM, Schmidt H et al (2010) Variants at APOE influence risk of deep and lobar intracerebral hemorrhage. Ann Neurol 68:934–943
2. Boulay AC, Saubaméa B, Declèves X, Cohen-Salmon M (2015) Purification of mouse brain vessels. J Vis Exp 105:e53208. doi:10.3791/53208
3. Braak H, Alafuzoff I, Arzberger T, Kretzschmar H, Del Tredici K (2006) Staging of Alzheimer disease-associated neurofibrillary pathology using paraffin sections and immunocytochemistry. Acta Neuropathol 112:389–404
4. Brenowitz WD, Nelson PT, Besser LM, Heller KB, Kukull WA (2015) Cerebral amyloid angiopathy and its co-occurrence with Alzheimer's disease and other cerebrovascular neuropathologic changes. Neurobiol Aging 36:2702–2708
5. Butterfield DA, Lange ML (2009) Multifunctional roles of enolase in Alzheimer's disease brain: beyond altered glucose metabolism. J Neurochem 111:915–933
6. Charidimou A, Martinez-Ramirez S, Shoamanesh A, Oliveira-Filho J, Frosch M, Vashkevich A et al (2015) Cerebral amyloid angiopathy with and without hemorrhage: evidence for different disease phenotypes. Neurology 84:1206–1212
7. Drummond E, Nayak S, Faustin A, Pires G, Hickman RA, Askenazi M et al (2017) Proteomic differences in amyloid plaques in rapidly progressive and sporadic Alzheimer's disease. Acta Neuropathol. doi:10.1007/s00401-017-1691-0
8. Esiri MM, Wilcock GK (1986) Cerebral amyloid angiopathy in dementia and old age. J Neurol Neurosurg Psychiatry 49:1221–1226
9. Ferreira CS, Papamichael K, Guilbault G, Schwarzacher T, Gariepy J, Missailidis S (2008) DNA aptamers against the MUC1 tumour marker: design of aptamer-antibody sandwich ELISA for the early diagnosis of epithelial tumours. Anal Bioanal Chem 390:1039–1050
10. Gauthier SA, Sahoo S, Jung SS, Levy E (2012) Murine cerebrovascular cells as a cell culture model for cerebral amyloid angiopathy: isolation of smooth muscle and endothelial cells from mouse brain. Methods Mol Biol 849:261–274
11. Gioia L, Vogt LJ, Freeman WM, Flood A, Vogt BA, Vrana KE (1998) PCR-based apolipoprotein E genotype analysis from archival fixed brain. J Neurosci Methods 80:209–214
12. Head D, Bugg JM, Goate AM, Fagan AM, Mintun MA, Benzinger T et al (2012) Exercise engagement as a moderator of the effects of APOE genotype on amyloid deposition. Arch Neurol 69:636–643
13. HUGO Gene Nomenclature Committee (2017) Gene family: sushi domain containing. http://www.genenames.org/cgi-bin/genefamilies/set/1179. Accessed 20 Mar 2017
14. Kim CJ, Shimakage M, Kushima R, Mukaisho K, Shinka T, Okada Y et al (2003) Down-regulation of *drs* mRNA in human prostate carcinomas. Hum Pathol 34:654–657
15. Liao L, Cheng D, Wang J, Duong DM, Losik TG, Gearing M et al (2004) Proteomic characterization of postmortem amyloid plaques isolated by laser capture microdissection. J Biol Chem 279:37061–37068
16. Mandybur TI (1975) The incidence of cerebral amyloid angiopathy in Alzheimer's disease. Neurology 25:120–126
17. Meindl A, Carvalho MR, Herrmann K, Lorenz B, Achatz H, Lorenz B et al (1995) A gene (SRPX) encoding a sushi-repeat-containing protein is deleted in patients with X-linked retinitis pigmentosa. Hum Mol Genet 4:2339–2346
18. Mirra SS, Heyman A, McKeel D, Sumi SM, Crain BJ, Brownlee LM et al (1991) The consortium to establish a registry for Alzheimer's disease (CERAD): part II. Standardization of the

neuropathologic assessment of Alzheimer's disease. Neurology 41:479–486
19. Nakamura T, Shinriki S, Jono H, Guo J, Ueda M, Hayashi M et al (2015) Intrinsic TGF-β2-triggered SDF-1-CXCR4 signaling axis is crucial for drug resistance and a slow-cycling state in bone marrow-disseminated tumor cells. Oncotarget 6:1008–1019. doi:10.18632/oncotarget.2826
20. Olsson B, Lautner R, Andreasson U, Öhrfelt A, Portelius E, Bjerke M et al (2016) CSF and blood biomarkers for the diagnosis of Alzheimer's disease: a systematic review and meta-analysis. Lancet Neurol 15:673–684
21. Paoletti AC, Parmely TJ, Tomomori-Sato C, Sato S, Zhu D, Conaway RC et al (2006) Quantitative proteomic analysis of distinct mammalian Mediator complexes using normalized spectral abundance factors. Proc Natl Acad Sci USA 103:18928–18933. doi:10.1073/pnas.0606379103
22. Pawłowski K, Muszewska A, Lenart A, Szczepińska T, Godzik A, Grynberg M (2010) A widespread peroxiredoxin-like domain present in tumor suppression- and progression-implicated proteins. BMC Genomics 11:590
23. Richards DB, Cookson LM, Berges AC, Barton SV, Lane T, Ritter JM et al (2015) Therapeutic clearance of amyloid by antibodies to serum amyloid P component. N Engl J Med 373:1106–1114. doi:10.1056/NEJMoa1504942
24. Sengüven B, Baris E, Oygur T, Berktas M (2014) Comparison of methods for the extraction of DNA from formalin-fixed, paraffin-embedded archival tissues. Int J Med Sci 11:494–499
25. Shimakage M, Kawahara K, Kikkawa N, Sasagawa T, Yutsudo M, Inoue H (2000) Down-regulation of drs mRNA in human colon adenocarcinomas. Int J Cancer 87:5–11
26. Tambe Y, Isono T, Haraguchi S, Yoshioka-Yamashita A, Yutsudo M, Inoue H (2004) A novel apoptotic pathway induced by the *drs* tumor suppressor gene. Oncogene 23:2977–2987. doi:10.1038/sj.onc.1207419
27. Tambe Y, Yoshioka-Yamashita A, Mukaisho K, Haraguchi S, Chano T, Isono T et al (2007) Tumor prone phenotype of mice deficient in a novel apoptosis-inducing gene, *drs*. Carcinogenesis 28:777–784. doi:10.1093/carcin/bgl211
28. Tasaki M, Ueda M, Obayashi K, Koike H, Kitagawa K, Ogi Y et al (2013) Effect of age and sex differences on wild-type transthyretin amyloid formation in familial amyloidotic polyneuropathy: a proteomic approach. Int J Cardiol 170:69–74. doi:10.1016/j.ijcard.2013.10.033
29. Ueda M, Horibata Y, Shono M, Misumi Y, Oshima T, Su Y et al (2011) Clinicopathological features of senile systemic amyloidosis: an ante- and post-mortem study. Mod Pathol 24:1533–1544. doi:10.1038/modpathol.2011.117
30. Viswanathan A, Greenberg SM (2011) Cerebral amyloid angiopathy in the elderly. Ann Neurol 70:871–880
31. Vrana JA, Gamez JD, Madden BJ, Theis JD, Bergen HR 3rd, Dogan A (2009) Classification of amyloidosis by laser microdissection and mass spectrometry-based proteomic analysis in clinical biopsy specimens. Blood 114:4957–4959